The Use of LS-DYNA to Simulate the Water Landing Characteristics of Space Vehicles

Benjamin A. Tutt
Systems Analyst
Irvin Aerospace Inc, Santa Ana California 92704

Anthony P. Taylor
Director, Business and Technical Development
Irvin Aerospace Inc, Santa Ana California 92704

Abstract

Irvin Aerospace, Inc. has been involved with the recovery/landing systems of re-entry and interplanetary space vehicles spanning a number of years. A significant aspect in the assessment of recovery and escape systems is the performance of such vehicles in the event of a water landing. One method used to reduce the loads imparted to the crew as the vehicle enters the water is to increase the drag area of the falling body. Increasing the drag area of the recovery system is a simple resolution, however, integration leads to an unfavorable increase in the total system mass and volume requirements. An alternative solution, utilized by the Apollo Earth Landing System, is to dictate the orientation of the vehicle prior to water impact. The results of an exhaustive test program showed that the accelerations experienced by the crew could be reduced by a factor of five simply by changing the vehicle water entry angle. This paper presents an application of the Eulerian-Lagrangian penalty coupling algorithm and multi-material ALE capabilities within LS-DYNA. Documented in the report are the results of a series of validation simulations undertaken by Irvin in an IRAD program to ascertain the capacity of LS-DYNA to replicate the water-landing characteristics of an Apollo Command Module and predict the performance of future landing systems

.

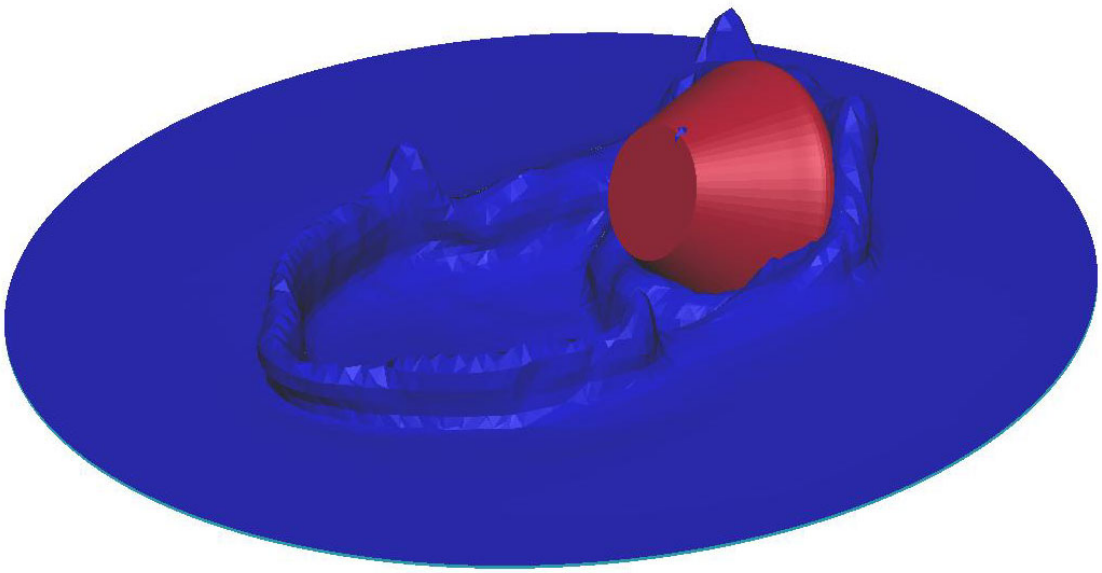

Introduction

The Earth Landing System (ELS) is an intrinsic component of any crewed space program. A safe and efficient ELS will reliably return a team of astronauts to Earth without unnecessarily increasing vehicle mass or volume.

The role of an ELS was illustrated during the pioneering stages of America's space program when first Mercury, Gemini, and then Apollo capsules were consistently decelerated from 24,000 mph to 0 mph. Figure 1 shows Apollo 17 under canopy before splashdown.

Figure 1: Apollo 17 just before splashdown

The success of the Mercury landing system was ultimately judged when John Glenn commented that the greatest acceleration he was subjected to was when Friendship 7 hit the recovery ship while being winched onboard. The role of an ELS evolved during the Space Shuttle program from a parachute and reorientation system to a winged body and landing gear.

In February 2001, NASA sought to identify feasible options for future space transportation. The Space Launch Initiative considered two programs- Next Generation Launch Technology and Next Generation Crew Rescue and Transfer, an Orbital Space Plane (OSP), a program that Irvin participated in. On January 2004, President Bush articulated a new 'Vision for Space Exploration in the 21st Century'. This vision encompasses a broad range of human and robotic mission to the Moon, Mars and beyond. The presidential directorate has resulted in the OSP partly morphing into and partially being superceded by a proposed Crew Exploration Vehicle.

Irvin Aerospace Inc (Irvin) has utilized LS-DYNA for many years for the analysis of fabric structures, including airbags, impact nets and other static fabric assemblies. Recent application of Fluid Structure Interaction (FSI) techniques within LS-DYNA for the analysis of parachutes, and

other dynamic events, at Irvin has highlighted the potential of the tool to predict spacecraft water impact loads.

This paper presents the results of an internal research and development effort by Irvin to ascertain the capacity of LS-DYNA to replicate the water-landing characteristics of an Apollo Command Module. Our purpose was to provide some validation of the code and our techniques that we might have confidence moving into future development programs. The paper discusses the experimental results from an original NASA test series undertaken during the Apollo program, describes the modeling approach and execution, and presents the correlation between test data and the analytical predictions.

Experimental Drop Test Program

National Aeronautics and Space Administration Technical Note D-3980 [1] documents the results of a drop test program conducted at the Langney Impacting Structures Facility during the late 1960s. The purpose of the experimental investigation was to determine water impact pressures, accelerations, and landing dynamics of a ¼ scale model of the Apollo spacecraft's Command Module (CM). At the time of the test series the Earth Landing System had been changed from a deployable heat shield to a passive system and a primary landing media of water.

The drop tests considered variations in CM pitch angle, roll angle, vertical and horizontal velocity, and mass when impacting the water. The drop test matrix covered impact perturbations due to changes in the vehicle's orientation caused by parachute motion and local wave slopes. Figure 2 displays the test apparatus; the model is in a pulled back position ready for release.

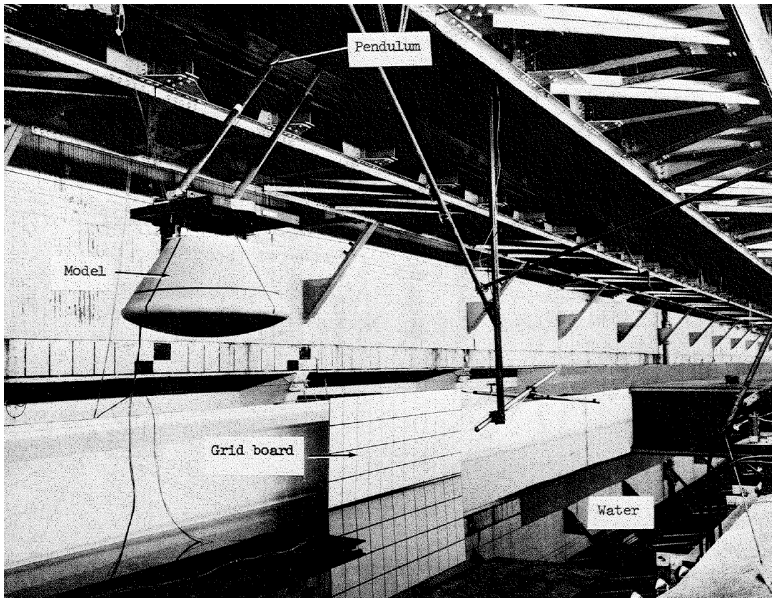

Figure 2: Original drop test set-up

Modeling Approach

LS-DYNA has the capability to simulate this type of dynamic event in many ways, including pure Lagrangian, coupled Lagrange and Euler, and Smooth Particle Hydrodynamics (SPH) methods. For the purpose of comparison with test data, a multi-material Eulerian formulation combined with an Eulerian-Lagrangian coupling algorithm was used as it is the most mature and thought to produce the best results.

A purely Lagrangian approach was considered but discarded, as although it may capture the initial impact accurately it was believed that numerical problems due to element distortion would limit its applicability to simulate post impact landing characteristics.

The SPH method was discarded due to the limited experience of the authors with this method and because of the expected increase in computational overhead associated with this algorithm. The SPH technique is a meshless Lagrangian method that enables materials such as fluids or gases that have very little strength in the shear direction to be simulated using a Lagrangian formulation.

The multi-material Eulerian formulation is classed as part of the Arbitrary- Lagrangian-Eulerian (ALE) solver within LS-DYNA. The ALE solver involves a Lagrangian step, where the mesh is allowed to move and a second step that advects (or moves) the element state variables back onto a reference mesh. The multi-material Eulerian formulation is a specific ALE case where the reference, or background, mesh velocity is zero. This formulation was chosen ahead of the more computationally efficient ALE moving mesh technique to allow simplification of boundary conditions and to enable the analyst to observe the entirety of the landing sequence as opposed to tracking the impact interface.

By combining the ALE solver with an Eulerian-Lagrangian penalty coupling algorithm, a structural or Lagrangian mesh can interact with a fluid, Eulerian mesh. This technique will allow an Apollo Command Module, constructed from a Lagrangian mesh to interact with an Eulerian based water impact site. LS-DYNA provides this feature through the addition of several simple cards.

Figure 3 identifies the vehicle axes, altitudes, and c.g. location. Table 1 displays the pertinent vehicle parameters, the ¼ scale model values were defined using typical Froude number scaling. The LS-DYNA model was constructed full-scale and all result data will be presented full-scale.

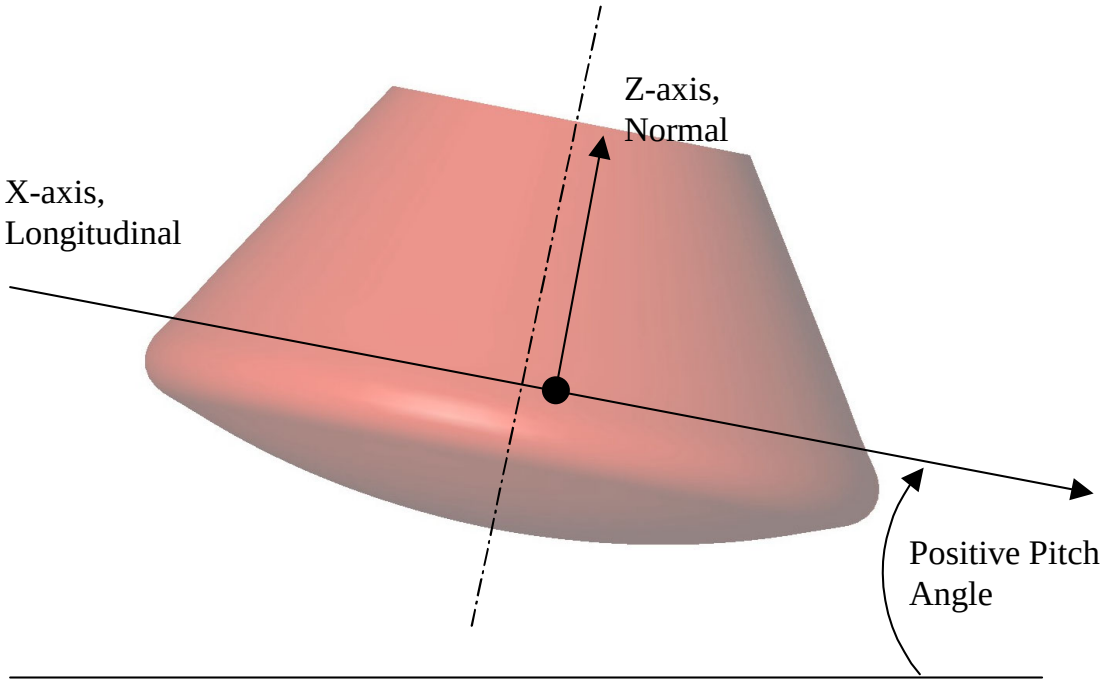

Figure 3: Vehicle axes definition

Parameter	¼ Scale Model	Full-Scale Vehicle
Mass	4.18 slugs	267.3 slugs
Diameter, max	37.9 in	151.5 in
Height	21.5 in	86.2 in
Moment of Inertia:		
Ixx	3.01 slug ft^2	3080 slug ft^2
Iyy	3.80 slug ft^2	3890 slug ft^2
Izz	4.01 slug ft^2	4100 slug ft^2

Table 1: Significant vehicle parameters

A number of small model development studies were performed to identify the most efficient and accurate modeling technique, a number of the more significant are discussed below:

Mesh geometry and density-
Previous FSI simulations conducted by the authors, containing a parachute in a high velocity fluid flow, occasionally exhibited a reversal of the flow at boundaries located perpendicular to

the fluid flow. To reduce the possibility of this reoccurring a cylindrical mesh was developed. Mesh density studies suggested a mesh of 6 in, in both the breadth and length dimensions and a depth of 4.5 in was sufficient to capture the impact. The mesh was graded both radially and with depth to aid computational efficiency. The air mesh is graded to a greater extent but is still quite fine at the impact zone; this enables visualization of the waves generated by the impact.

Water density-depth initialization-
A depth of 200 in was found to be sufficient to allow accurate and distinct pressure initialization of the water. Boundary conditions were specified to eliminate any reflections.

Air pressurization-
An air pressurization study was conducted to confirm that the magnitude of the pressure in the air was not important and that the relative difference in pressure between the air and the water was the necessary parameter.

Vehicle starting location-
A review of the starting location of the vehicle was performed. It was clear that the vehicle would need to fall from a height great enough to allow the surrounding air to become energized but not so high as to increase the run-time unnecessarily. It was found that a c.g. location 120 in above the water surface was adequate for all vehicle pitch attitudes and initial velocities.

Hourglass-
The most influential parameters were those on the hourglass card. Hourglass control types 1, standard viscous form, and 6, the assumed strain co-rotational stiffness form, were considered. Control type 6, which defaults to a viscous form and is scaled according to material viscosity when used with the *mat_null material model, produced satisfactory results. However, the standard viscous form, combined with a reduced hourglass coefficient of 1.0e-04, produced considerably better results.

Rigid body definition-
As the post impact landing characteristics were of importance during this study it was critical that the vehicle's moments of inertia were accurately captured. The simplest way of achieving this is to utilize the *part_inertia card and a rigid body description. The authors believe the rigid body definition is valid and this is reinforced by comments in the NASA Technical Note.

Advection algorithms-
LS-DYNA incorporates both first and second order accurate advection algorithms. First order accurate solutions can be thought of as generally smoothing a solution and reducing peak values. A comparison of first order (donor cell) and second order (Van Leer MUSCL) accurate advection algorithms resulted in almost identical results. All proceeding simulations were conducted using the first order accurate technique.

Equation of state (EOS)-
Linear-polynomial and Gruneisen EOS's where evaluated. Both definitions yielded very similar results, the Gruneisen EOS was chosen for the remaining simulations.

Figure 4 depicts the computational mesh used for the validation simulations. The mesh consisted of 150,000 solid elements and 5,000 shell elements. The simulations were performed on a high-end PC running LS-DYNA version 970.

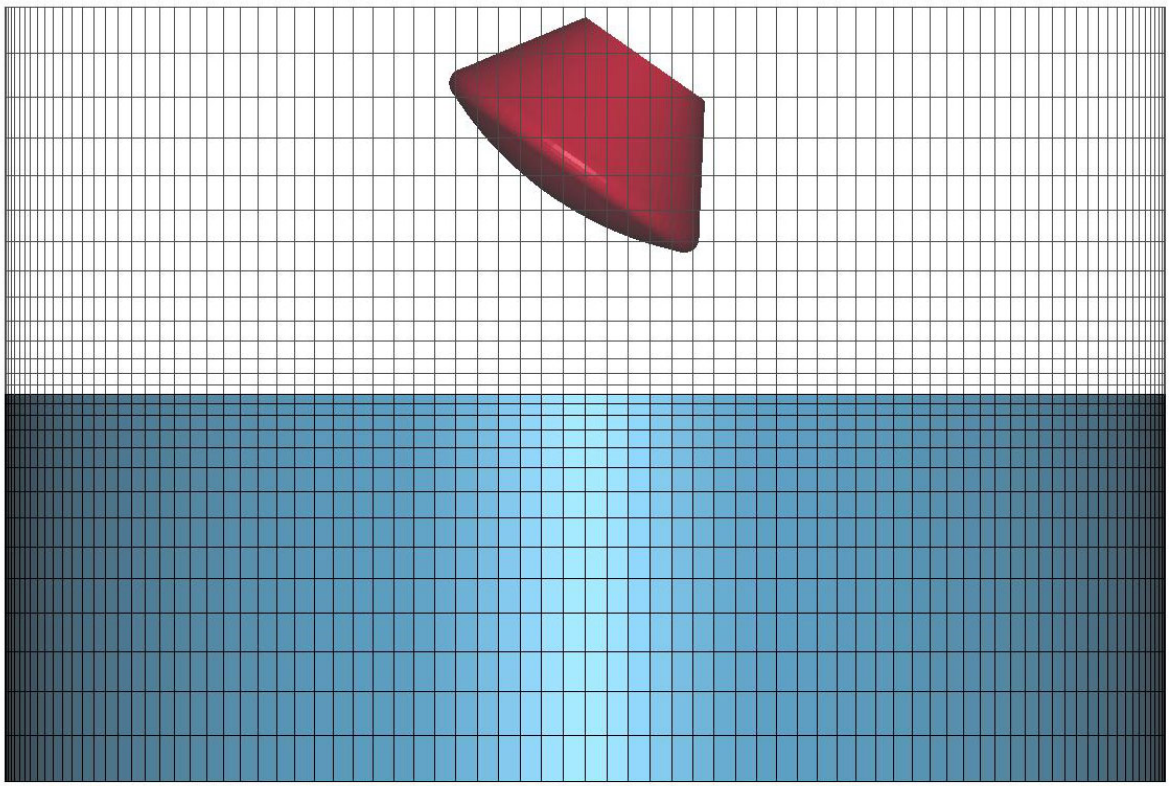

Figure 4: Computational mesh

A series of eight simulations were conducted with pitch angles varying between 14 and 39 degrees. Local accelerations at the c.g. of the vehicle were obtained by using the rotation and global acceleration data from the rbdout file, this data could then be directly compared with the test data.

Results

The majority of drop tests were conducted at vertical velocities between 30-32 ft/s. It is believed that this elevated rate of descent was used as a 'worst case' impact to account for the possible failure of one of the three parachutes, as happened during the return of Apollo 15, see Figure 5.

Figure 5: Apollo 15 with two canopies

Table 2 details the impact conditions and the results from the eight drop tests. Table 3 contains the same scenarios simulated with LS-DYNA.

Vertical Velocity (ft/s)	**Horizontal Velocity** (ft/s)	**Landing Attitude**			**Normal Accl.** (g)	**Longitudinal Accl.** (g)	**Angular Accl.** (g)
		Pitch (deg)	Roll (deg)	Yaw (deg)			
29.8	0	39	0	0	4.1	1.9	29
30.2	0	35	0	0	5.3	2.4	29
30.4	0	30	0	0	7.2	2.9	54
31.0	0	27	0	0	8.3	3.5	60
31.2	0	25	0	0	12.4	4.9	72
31.6 31.6 31.7	0	20	0	0	13.9 15.1 15.4	5.1 4.7 5.6	97 98 112
31.4	0	18	0	0	19.7	6.2	97
31.8	0	14	0	0	31.1	6.3	155

Table 2: Original drop test results

The three drop tests at 20 degrees pitch were included to give an indication of the spread of data from similar drops. The maximum variation in results obtained from identical impact scenarios was just over 10%.

Vertical Velocity (ft/s)	Horizontal Velocity (ft/s)	Landing Attitude			Normal Accl. (g)	Longitudinal Accl. (g)	Angular Accl. (g)
		Pitch (deg)	Roll (deg)	Yaw (deg)			
29.7	0	39	0	0	5.2	2.2	37
30.4	0	35	0	0	6.7	2.3	41
30.4	0	30	0	0	7.9	2.3	46
31.1	0	27	0	0	9.4	2.9	57
31.3	0	25	0	0	9.9	3.3	69
31.5	0	20	0	0	15.8	5.1	111
31.3	0	18	0	0	19.0	5.8	126
31.5	0	14	0	0	25.1	6.1	136

Table 3: LS-DYNA simulation results

The individual data points reported in Table 3 suggested a high level of correlation. The NASA Technical Note included a limited number of acceleration time history traces, however the plots were not of great quality and no information regarding the use or extent of filtering was included, for this reason only general comparisons have been made.

Figure 6 displays both the normal and longitudinal acceleration time history data for the 18 degree impact simulation. The peak acceleration values and the total time period compare very well with the drop test data, presented in Table 2.

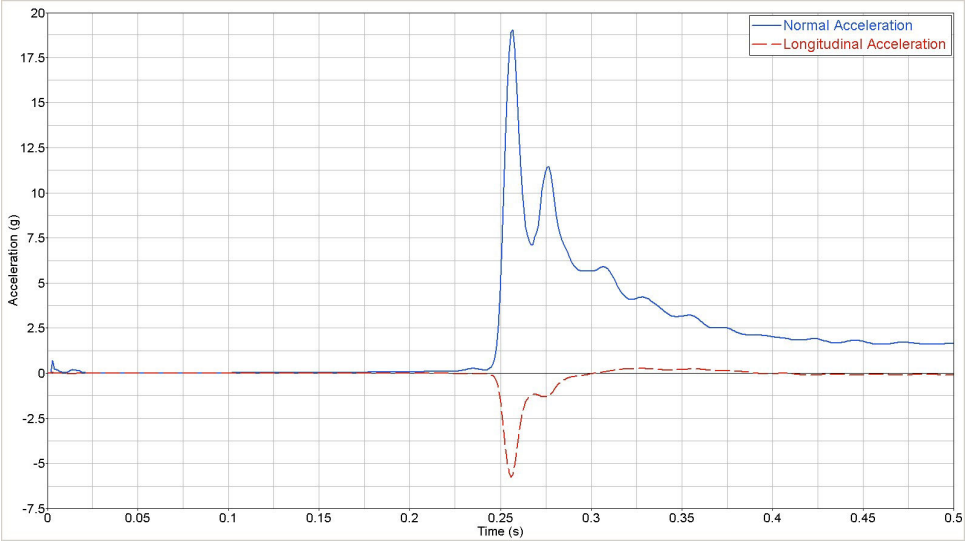

Figure 6: Acceleration time history data from the 18 degree pitch impact

To illustrate the validity of the model over a broad range of pitch angles Figure 7 displays the acceleration time history data for the 35 degree impact pitch angle. Again, the peak values and time period compare incredibly well with the test data.

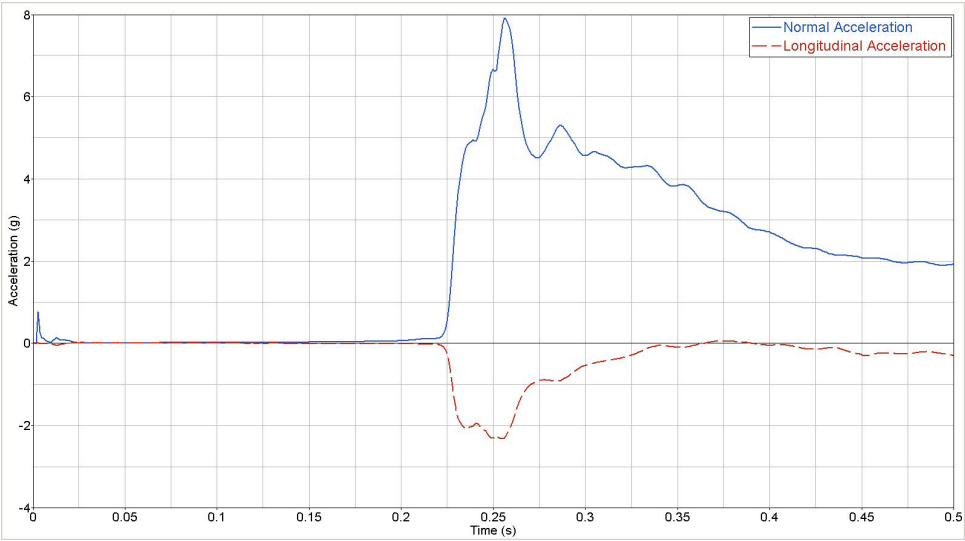

Figure 7: Acceleration time history data from the 35 degree pitch impact

Figure 8 illustrates the time history data of the vehicle's pitch rotation, angular acceleration and vertical velocity for both the 18 and 35 degree impacts. The units of vertical velocity are in/s in Figure 8 to allow easier graphical identification.

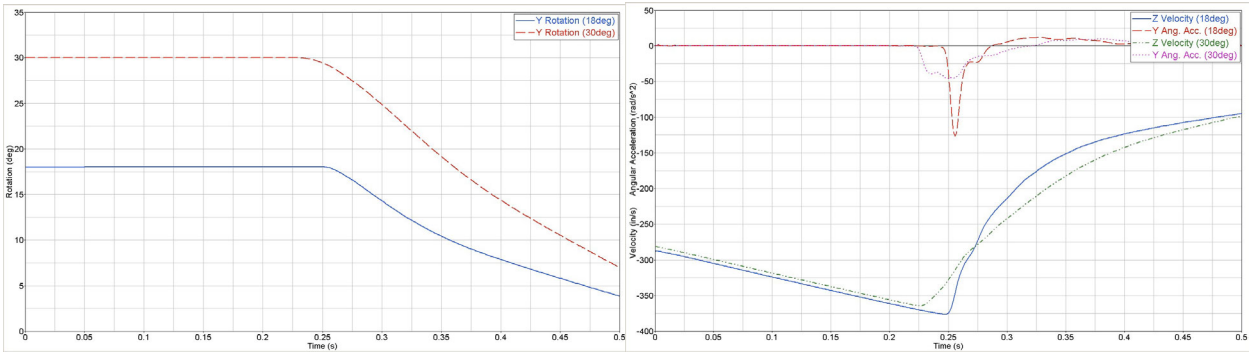

Figure 8: Additional time history data from the 18 and 35 degree pitch impacts

Figure 8 allows the landing performance of the vehicle to be tracked throughout the water landing, although, perhaps a better way of understanding the vehicle's motion during the impact is to visualize it. Figure 9 shows four frames depicting the Apollo CM impacting the water at a pitch angle of 35 degrees. The simulation graphic presents fluid density, with red representing high density (water) and blue, low density (air).

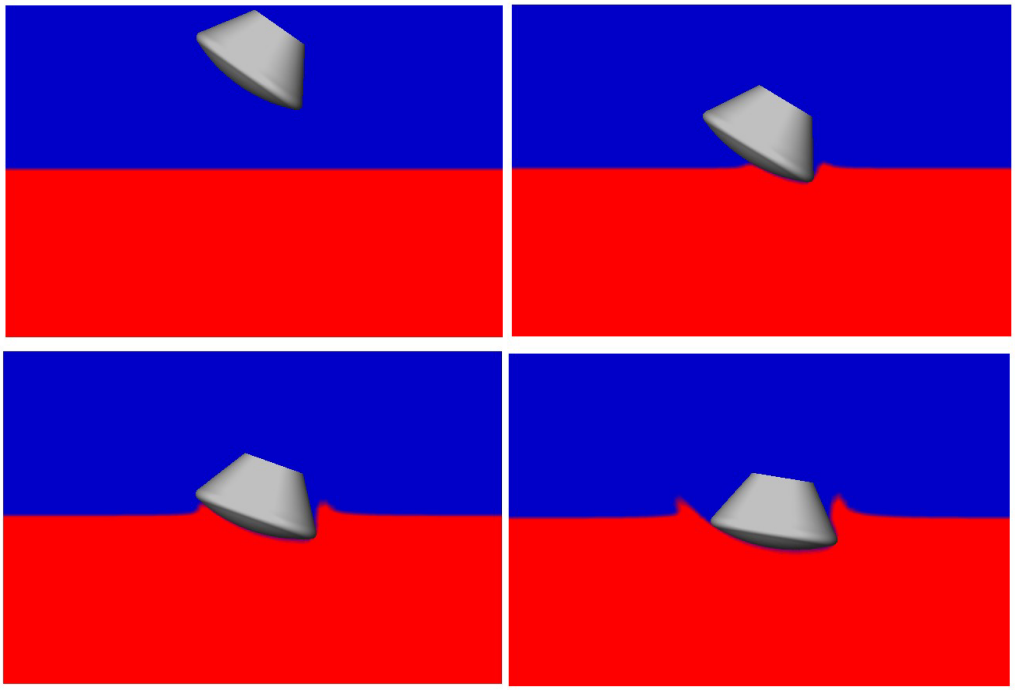

Figure 9: Fluid density plot from the 35 degree pitch impact

Figure 10 provides an overview of the results presented in Tables 2 and 3. Test data is depicted with blue cylinders and simulation results with red cylinders. The graph compares peak normal accelerations and illustrates how well the LS-DYNA predictions follow the overall trend of test results.

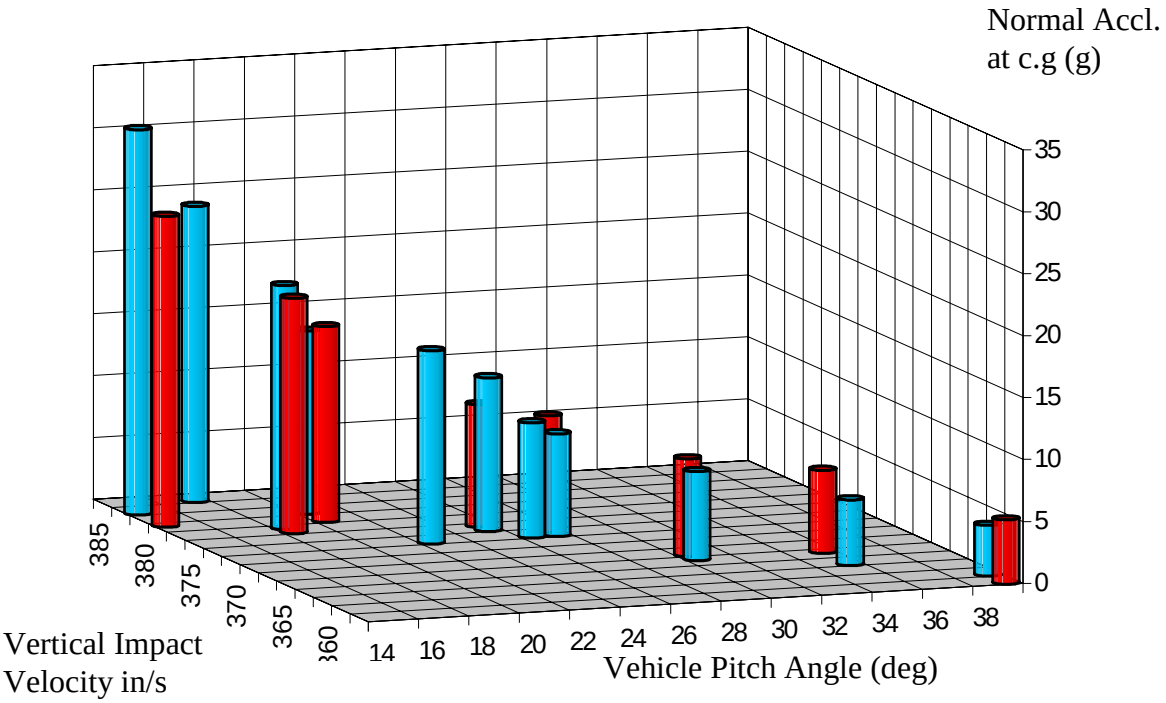

Figure 10: Comparison of test data and analytical predictions

In addition to the scenarios described above a number of supplementary simulations were conducted.

Two simulations with increased vehicle mass were undertaken. The results are presented in Figure 11. As would be expected, the heavier vehicles experience a reduction in peak acceleration values.

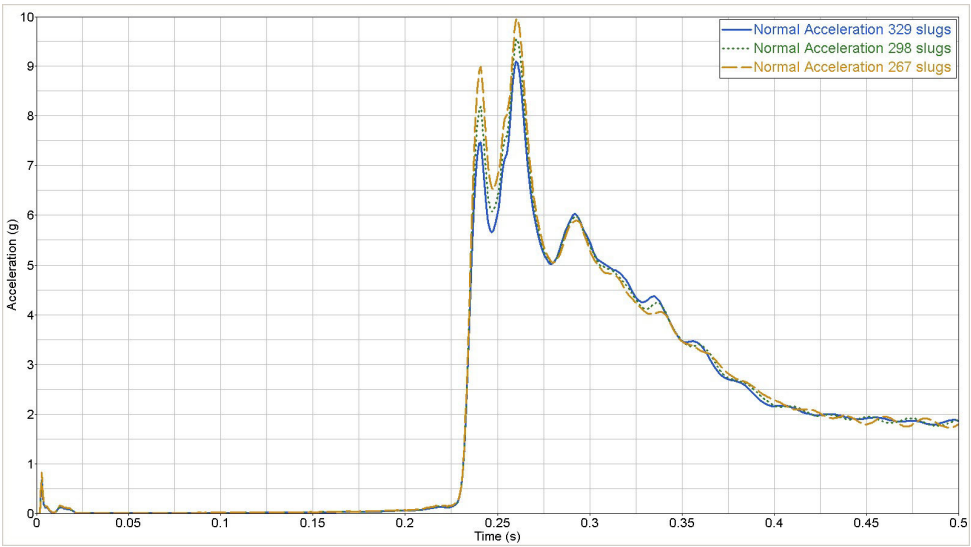

Figure 11: Acceleration time history data from vehicles of differing mass

Several simulations were conducted with the Apollo CM possessing a horizontal velocity. Figure 12 illustrates the fluid density plots for a CM at 20 degrees pitch angle, 30.4 ft/s vertical velocity and 50 ft/s horizontal velocity.

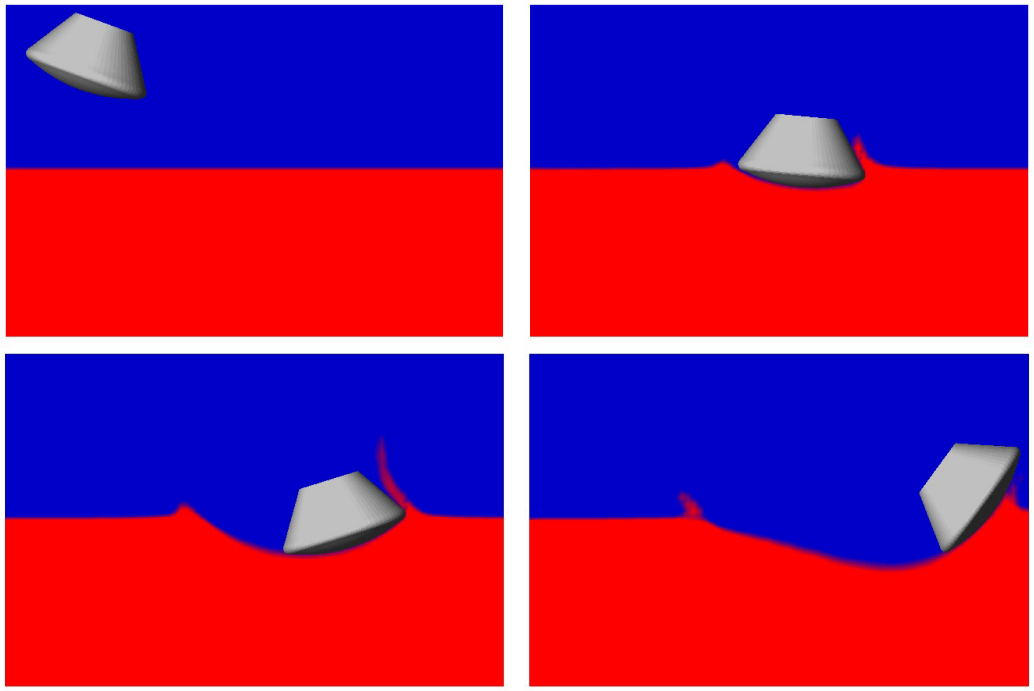

Figure 12: Fluid density plot of an impact with horizontal velocity

This particular landing scenario is best visualized by an iso-surface plot, Figure 13 highlights the size of the wave/splash produced by the impact.

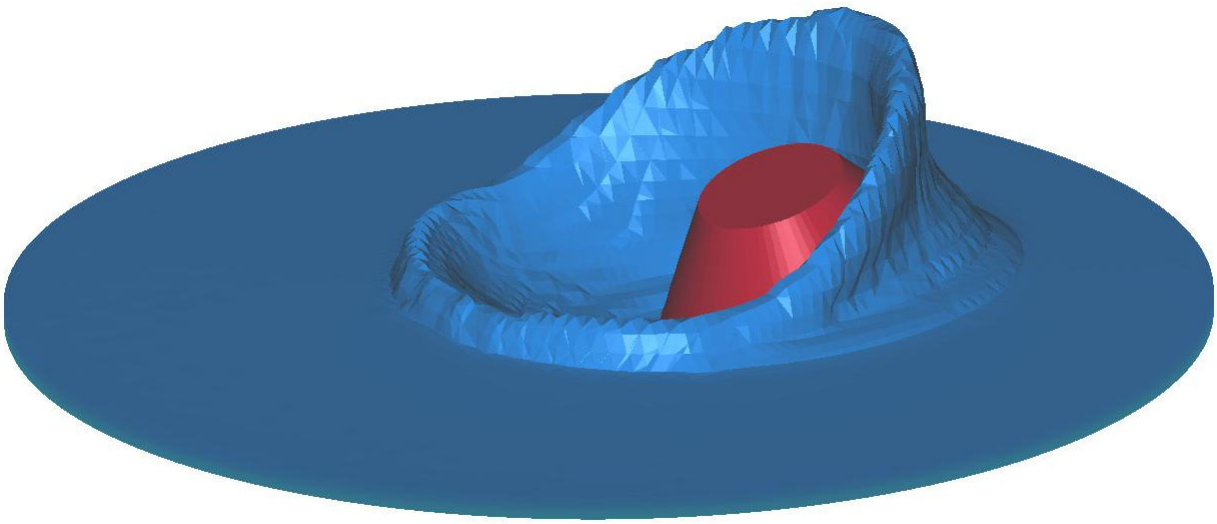

Figure 13: Iso surface plot of an impact with horizontal velocity

Conclusions

We find the results of this internally funded validation study very compelling. It should be noted that these simulations are relatively simple, but have clearly proved the value of such a tool and the methodology applied. It was noted during the study that water impact simulations involving the Command Module at small pitch angles tended to underpredict the impact accelerations. After reviewing the NASA Technical Note that documented the test series it became evident that drop tests involving small pitch angles caused the heat shield to vibrate. This phenomenon resulted in pronounced oscillations in the normal acceleration traces and produce inadvertently high accelerations. It was also noted that these oscillations decreased as the pitch attitude of the vehicle was increased. In tests of a model with a rigid heat shield, not reported, the oscillations did not occur.

Further levels of complexity can be introduced to the model as well as scrutinizing the results further. Current and planned work includes more in-depth analysis of the vehicle impact pressures, a fully deformable vehicle and floatation studies.

The application of the multi-material Eulerian formulation and a penalty based Lagrangian-Eulerian coupling algorithm was shown to accurately capture the water landing while incurring an acceptable computational overhead. Further investigation of the SPH technique is planned along with a combination of SPH and mesh free methods.

We are convinced that this tool can play an important role in the design of future Earth Landing Systems and provide a significant tool for guiding a more concise and focused development and drop test program.

References

[1] Stubbs, S.M., “Dynamic Model Investigation of Water Pressures and Accelerations Encountered During Landings of the Apollo Spacecraft”, NASA TN D-3980, (1967).

[2] Hallquist, J.O., “LS-DYNA Theoretical Manual”, LSTC Livermore, (1998).

[3] Taylor, A.P., Tutt, B.A., and Sanders, J “The Application of Explicit Finite Element Analysis and Fluid/Structure Simulations as They Apply to Escape and Recovery Systems” SAFE (2003).